

Molecular Structure and UV Absorption Spectra of OH and NH₂ Derivatives of Dodecamethylcyclohexasilane: A Combined Experimental and Computational Study

Harald Stueger, Gottfried Fuerpass, Judith Baumgartner, Thomas Mitterfellner, and Michaela Flock

Institute of Inorganic Chemistry, Graz University of Technology, Stremayrgasse 16, 8010 Graz, Austria

Reprint requests to Prof. Dr. Harald Stüger. Fax: +43-316-8701. E-mail: harald.stueger@tugraz.at

Z. Naturforsch. 2009, 64b, 1598–1606; received August 19, 2009

Dedicated to Professor Hubert Schmidbaur on the occasion of his 75th birthday

The monofunctionalized cyclohexasilanes XSi₆Me₁₁ [X = -OH (**2**); -NH₂ (**3**)] are easily accessible from XSi₆Me₁₁ and H₂O/Et₃N or NH₃, respectively. The crystal structure of **2** as determined by single crystal X-ray crystallography exhibits the cyclohexasilane ring in chair conformation with the OH group in an unusual equatorial position due to intermolecular hydrogen bonding. Full geometry optimization (B3LYP/6-31+G*) of the gas-phase structures of **2** and **3** affords six minima on the potential energy surface for *chair*, *twist* and *boat* conformers with the heterosubstituents either in axial or equatorial positions all being very close in energy. According to time-dependent DFT B3LYP/TZVP calculations contributions of several conformers to the observed solution UV absorption spectra of dodecamethylcyclohexasilane (**1**), **2** and **3** need to be considered in order to achieve satisfactory agreement of calculated and experimental data.

Key words: Cyclopolysilanes, Aminosilanes, Silanols, UV Absorption Spectra, Molecular Structure

Introduction

In oligo- and polysilanes delocalization of σ (Si–Si) electrons over a network of silicon atoms gives these molecules a variety of properties reminiscent of conjugated organic π electrons [1], such as unusually long-wavelength UV absorption maxima, low ionization energies, non-linear optical behavior [2], fluorescence [3] or photochemical activity. σ -Delocalization in Si–Si-bonded compounds has also been treated theoretically on various levels of theory including simple Hückel, semiempirical, *ab initio* and DFT methods [4]. In addition, pronounced substituent effects on polysilane properties, such as bathochromically shifted UV/Vis absorption maxima are observed, when unsaturated organic side groups like phenyl, vinyl or acetylene moieties or atoms with π -symmetric lone pairs of electrons like halogens, O or N are linked directly to the Si–Si framework [5].

A series of recent investigations revealed, that the UV/Vis absorption spectra and other photophysical

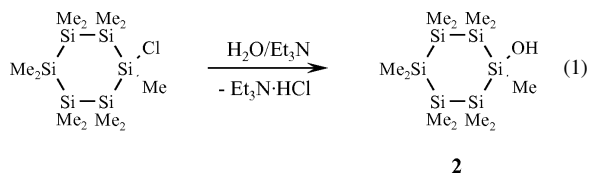
properties of open-chained polysilanes are additionally influenced by the silicon backbone conformation [6]. Since oligo- and polysilanes like the permethylated derivatives Si_nMe_{2n+2} are present as mixtures of rapidly interconverting conformational isomers at least at room temperature, several conformers with distinct spectral properties usually contribute to the "normal" absorption in solution [7]. According to a recently published Raman spectroscopy and DFT study [8] on the conformational composition of dodecamethylcyclohexasilane (**1**) detecting three stable conformers of the permethylated cyclohexasilanyl ring, a similar situation may be encountered in the UV absorption spectra of other cyclic polysilanes.

Herein we report on the computational assignment of the solution UV absorption spectra of **1** using time-dependent DFT. Furthermore, the structural properties and UV/Vis absorption characteristics of the monofunctionalized derivatives Si₆Me₁₁OH (**2**) and Si₆Me₁₁NH₂ (**3**) will be presented in order to explore the impact of the heterosubstituents on the cyclohexasilane framework.

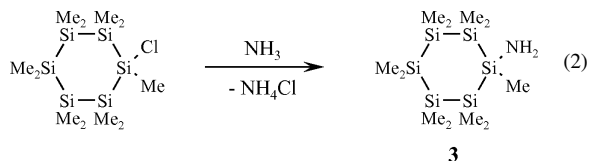
Results and Discussion

Synthesis

Hydroxyundecamethylcyclohexasilane (**2**) has already been prepared in 1989 by the hydrolysis of BrSi₆Me₁₁ [9], but no crystal structure has been published so far. In the present paper **2** was synthesized using a slightly modified procedure starting from ClSi₆Me₁₁ under employment of Et₃N as an auxiliary base in order to obtain higher yields (Eq. 1).



Compound **3**, the first cyclosilane derivative containing an NH₂ group directly attached to silicon, is easily prepared in yields > 90 % from ClSi₆Me₁₁ with an excess of anhydrous NH₃ (Eq. 2).



Care has to be taken in the course of the synthesis to avoid even traces of moisture, because **3** is easily hydrolyzed to give the corresponding silanol **2** as an impurity, which cannot be separated from the desired product. Ring scission or condensation reactions in the course of the synthesis of **3** by loss of NH₃ to give silazanes do not cause any problems. Crystals of **3** can be stored at room temperature for several weeks without any noticeable decomposition. Analytical data (see Experimental Section) obtained for **3** are consistent with the proposed structure. Attachment of the NH₂ group to the cyclohexasilanyl ring causes a marked downfield shift of the α -Si resonance line relative to Si₆Me₁₂ [10] by 27.2 ppm in the ²⁹Si NMR spectrum.

Structural Characterization

Compound **3** crystallizes in a monoclinic space group with nearly identical cell parameters as recently obtained for **1** [11]. Unlike the OH group in **2** the NH₂ group in **3** turned out to be disordered over all twelve possible positions. Thus, a satisfactory solution and refinement of the crystal structure was not possible.

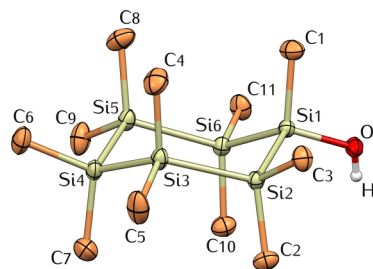


Fig. 1. Molecular structure of **2** (displacement ellipsoids at the 50 % probability level; hydrogen atoms omitted for clarity, except for O-H). Selected bond lengths (Å) and angles (deg) with estimated standard deviations: Si(1)–O(1) 1.6706(12), Si(1)–Si(6) 2.3506(7), Si(1)–Si(2) 2.3505(8), Si(2)–Si(3) 2.3449(7), Si(3)–Si(4) 2.3419(7), Si(4)–Si(5) 2.3372(8), Si(5)–Si(6) 2.3394(7), Si(1)–C(1) 1.870(2), Si(2)–C(3) 1.886(2), Si(2)–C(2) 1.886(2), Si(3)–C(4) 1.885(2), Si(3)–C(5) 1.888(2), Si(4)–C(7) 1.884(2), Si(4)–C(6) 1.887(2), Si(5)–C(8) 1.886(2); Si(5)–C(9) 1.890(2), Si(6)–C(10) 1.886(2), Si(6)–C(11) 1.886(2); Si(6)–Si(1)–Si(2) 109.13(2), Si(3)–Si(2)–Si(1) 111.82(3), Si(4)–Si(3)–Si(2) 113.79(3), Si(5)–Si(4)–Si(3) 110.14(3), Si(4)–Si(5)–Si(6) 111.77(3), Si(5)–Si(6)–Si(1) 111.31(3), O(1)–Si(1)–Si(2) 110.59(5), O(1)–Si(1)–Si(6) 111.15(5), O(1)–Si(1)–C(1) 104.28(7), C–Si–C (mean) 107.8.

Compound **2** is rather reluctant to crystallize. Low-temperature recrystallization of **2** from pentane eventually afforded colorless crystals suitable for X-ray crystal structure analysis. The crystals, grown very slowly over a few months at –30 °C, undergo a phase transition upon warming to room temperature. At room temperature, **2** is a waxy, colorless solid. Therefore, the crystal structure was determined at 100 K, after the crystal was mounted at –50 °C. A drawing of the molecular structure of **2** is shown in Fig. 1 together with a listing of selected bond lengths and angles.

Compound **2** crystallizes in the monoclinic space group *P2₁/c* with three independent molecules in the asymmetric unit. The cyclohexasilane ring adopts a slightly distorted chair conformation. Average Si–Si distances of 2.344 Å are close to the one in elemental silicon of 2.35 Å, and to those of related cyclohexasilane derivatives [12]. Compound **2** exhibits an unexceptional Si–O bond length of 1.671 Å, which is close to the average Si–OH distance for silanols of 1.64 Å [13] and nearly identical to the Si–O distance in 1,3- and 1,4-(HO)₂Si₆Me₁₀ [12b–d]. This value is markedly shorter than the Si–O bond length of 1.77 Å estimated from the sum of the covalent radii of silicon and oxygen, what at least in part can be attributed to the polarity of the Si–O bond [14]. Due to the presence of the OH substituent the Si(1)–C(1) bond is also

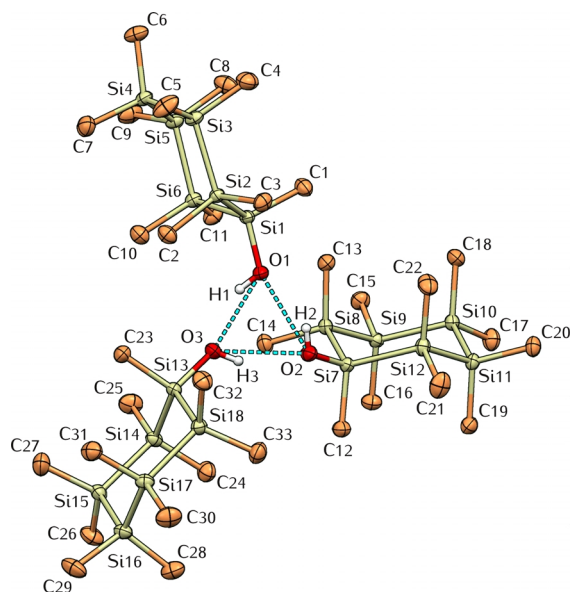


Fig. 2. Molecular aggregates formed by three crystallographically independent molecules of **2** (hydrogen atoms omitted for clarity, except for O-H). Oxygen atoms are associated to form a triangle due to intermolecular hydrogen bonding. $d(\text{O}\cdots\text{O}) = 2.781 \pm 0.026 \text{ \AA}$; $\angle(\text{O1}, \text{O2}, \text{O3}) = 59.0^\circ$, $\angle(\text{O2}, \text{O3}, \text{O1}) = 60.8^\circ$, $\angle(\text{O3}, \text{O1}, \text{O2}) = 60.2^\circ$.

significantly shortened by 0.017 \AA as compared to the average Si–C bond distance of 1.887 \AA observed for the residual Si–C bonds. This feature is also apparent in the calculated gas-phase structures of **2** mentioned below.

The geometry around the silicon atoms of **2** is approximately tetrahedral. The average Si–Si–Si bond angles are close to the respective angles found in other cyclohexasilane structures [12, 15]. The OH substituent in **2** occupies an equatorial position at the cyclohexasilane ring, what is atypical for small heterosubstituents attached to the Si₆ cycle. The reason for this unusual feature can be found in the packing of the individual molecules. The asymmetric unit of **2** contains three individual molecules, oriented in a propeller-like fashion around a triangle of oxygen atoms, which are linked to each other *via* hydrogen bonds (Fig. 2). For steric reasons this solid-state structure can only be adopted with equatorial OH groups.

It is interesting to compare the structure of **2** with that of 1,3-(HO)₂Si₆Me₁₀ [12c]. In crystals of the latter, the molecules are linked by intermolecular O→H bonds to infinite chains, due to the presence of axially placed OH groups. Hydrogen bonding in solid **2** is also reflected by the infrared O–H stretching fre-

Table 1. Absorption data for **1–3** (C₆H₁₂ solution, $c = 10^{-4} \text{ mol L}^{-1}$).

Compound	$\lambda_{\text{max,abs}}$, nm (ϵ , L mol ⁻¹ cm ⁻¹)	Reference
1	258 (1200)	[17]
	231 (5900)	
2	270 (880)	this work
	234 (4700)	
	284 (860)	
3	284 (860)	this work
	227 (8900)	

quency values. IR spectra of **2** recorded in diluted CCl₄ solution exhibit a sharp peak at 3680 cm^{-1} typical for free Si–OH groups, while in the solid-state spectrum (recorded as a KBr pellet) a broad peak at about 3420 cm^{-1} dominates, characteristic for hydrogen-bonded Si–OH [16].

UV Spectra and assignment

The UV absorption spectra of **1**, **2** and **3** (Table 1, Figs. 6–8) exhibit several overlapping bands at the low-energy side. Upon introduction of the OH and NH₂ group, respectively, the first absorption maximum is red-shifted from 256 nm for **1** [17] to 270 nm for **2** and 284 nm for **3**. Similar bathochromic shifts upon heterosubstitution were observed for permethoxycyclopolysilanes [Si(OMe)₂]_n [18] and 2-substituted derivatives of heptamethyltrisilane [19]. UV absorption maxima of highly polymeric alkoxy-substituted polysilanes were also found to be red-shifted relative to their alkyl-substituted analogs [20].

The low-energy absorption bands appearing in the UV spectra of permethylcyclopolysilanes (SiMe₂)_n are generally assigned to $\sigma \rightarrow \sigma^*$ -type excitations of highly delocalized Si–Si σ electrons within the Si–Si backbone [21]. In order to achieve a tentative assignment of the low-energy UV absorption bands, compounds **1–3** were treated theoretically using density functional methods. Figs. 3, 5 and 6 show the DFT (B3LYP/6-31+G*)-optimized geometries, relative energies and time-dependent DFT B3LYP/TZVP UV low-energy absorption bands.

Compound **1** exhibits three minima on the potential energy surface corresponding to the chair, twist and boat conformations with relative energies of 0.0 , 7.8 and 11.4 kJ mol^{-1} , respectively (Fig. 3). Due to these small energy differences and to the low barriers of internal rotation usually observed around Si–Si bonds, all conformers should be reasonably populated at room temperature and, therefore, contribute to the experimental properties. This expectation is fully confirmed

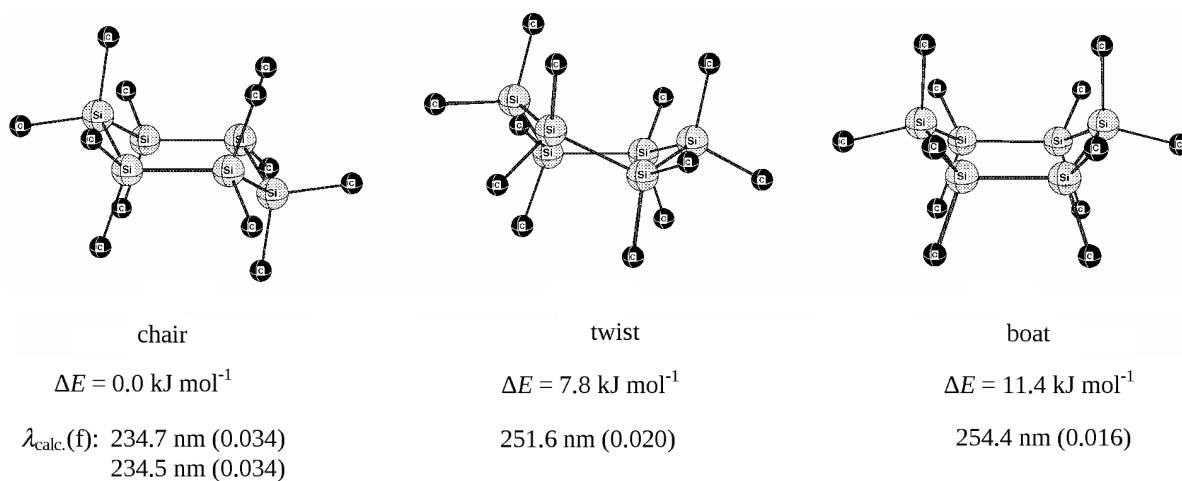


Fig. 3. DFT (B3LYP/6-31+G*)-optimized geometries, relative energies and time-dependent DFT B3LYP/TZVP UV long-wavelength absorption bands for **1** (oscillator strengths in parentheses).

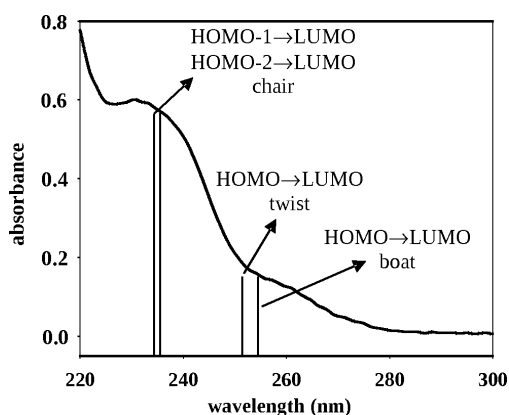


Fig. 4. Assignment of the experimental UV absorption spectrum by time-dependent DFT B3LYP/TZVP electron transitions for **1**, assuming contributions of different conformers.

by recent Raman spectroscopy studies showing contributions of at least two conformers to the experimental spectra recorded in solution at room temperature [8].

Experimental UV absorption data of **1** are also consistent with contributions of several conformational isomers to the shape of the overall spectrum (Fig. 4). The longest-wavelength absorption band attributed to the HOMO→LUMO transition in twist- and boat-**1** is calculated at 251.6 and 254.4 nm, respectively, perfectly in agreement with the absorption maximum of the experiment (258 nm). In the chair conformer (D_{3d} symmetry) the HOMO→LUMO transition is symmetry forbidden. Thus, the first observable absorption bands are predicted close to the experimental

232 nm maximum at 234.7 nm and 234.5 and assigned to HOMO-1→LUMO and HOMO-2→LUMO transitions, and the experimental spectrum is a nearly perfect superposition of the calculated spectra of the individual conformers.

The monosubstituted derivatives **2** and **3** both exhibit six local minima (Figs. 5 and 6). Conformers with the cyclohexasilanyl ring in a *chair* conformation are generally predicted to be more stable than the corresponding *twist* or *boat* forms. An axial position of the heterosubstituent turned out to be energetically favored with respect to an equatorial site. Calculated energy differences are small paralleling the results obtained for Si₆Me₁₂. Contributions of several conformers to the UV absorption spectra, therefore, need to be invoked also in the case of **2** and **3** in order to achieve a correct assignment of the observed absorption maxima.

The band at 270 nm observed in the experimental spectrum of **2** is straightforwardly assigned to the HOMO→LUMO transition in the *twist* and *boat* conformers calculated at 264.4, 261.6 and 263.8 nm, respectively, while the broad second maximum appearing at 234 nm can be attributed primarily to contributions of the axial and the equatorial *chair* conformers, where a zero transition moment is calculated for the HOMO→LUMO transition, causing a significant shift of the longest-wavelength absorption bands (HOMO-1,2→LUMO transitions) to 245.8, 242.2, 241.6 and 235.7 nm, respectively (Fig. 7).

Due to considerable interactions of the nitrogen lone pair of electrons with the permethylated cyclohexa-

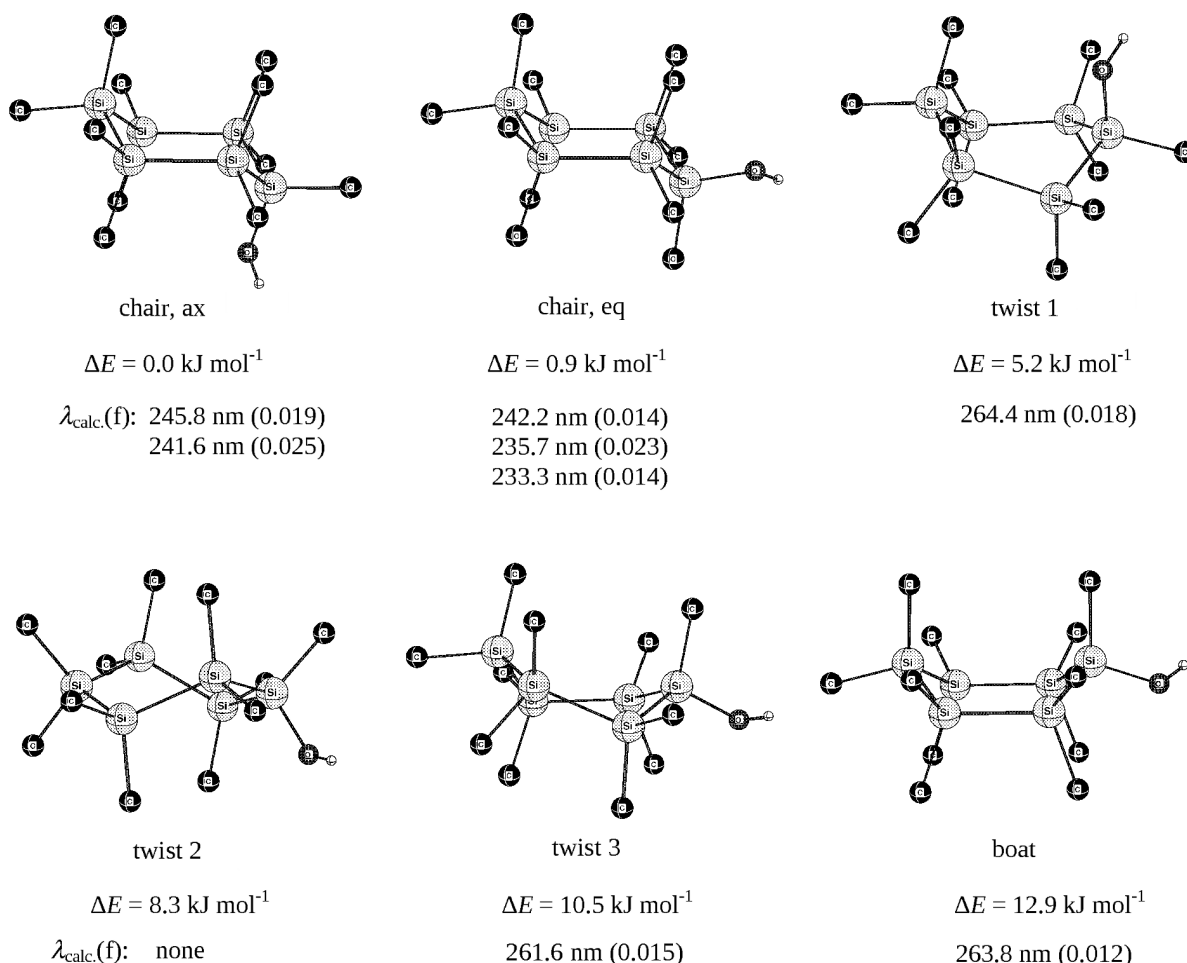


Fig. 5. DFT (B3LYP/6-31+G*)-optimized geometries, relative energies and time-dependent DFT B3LYP/TZVP UV long-wavelength absorption bands for **2** (oscillator strengths in parentheses).

silanyl ring twelve non-forbidden electron transitions with excitation wavelengths > 220 nm are calculated for the six conformers of **3** giving rise to a poorly resolved experimental absorption spectrum (Fig. 8). In this case the HOMO→LUMO transition in the equatorial chair and two of the twist conformers are predicted to contribute to the longest wavelength absorption band near 280 nm.

Substituent effects as apparent in the absorption spectra of **1–3** are consistent with earlier interpretations in terms of σ - n interactions between the lone pair of electrons on the heterosubstituent and the Si–Si backbone electronic structure, leading to a potential reduction of the HOMO-LUMO gap [18, 22]. This picture is fully supported by our computational results, as demonstrated by the shape and energy of the calculated

frontier orbitals involved in the longest-wavelength electron transitions of **1–3** (Fig. 9).

In all cases an electron is excited from the HOMO with predominant σ (Si–Si) contribution, which is delocalized over the cyclohexasilanyl framework, to a LUMO with high σ^* (Si–Si) character. The corresponding MO's of **2** and **3** additionally exhibit contributions of substituent lone pairs giving rise to significant reduction of the HOMO-LUMO gap from 5.79 eV in **1** to 5.57 eV in **2** and 5.25 eV in **3**. The importance of σ - n conjugation becomes particularly apparent in the HOMO of **3**, where effective mixing of σ (Si–Si) and n (N) orbitals raises the orbital energy by 0.5 eV as compared to **1**, what is almost exclusively responsible for the observed reduction of the excitation energy and the

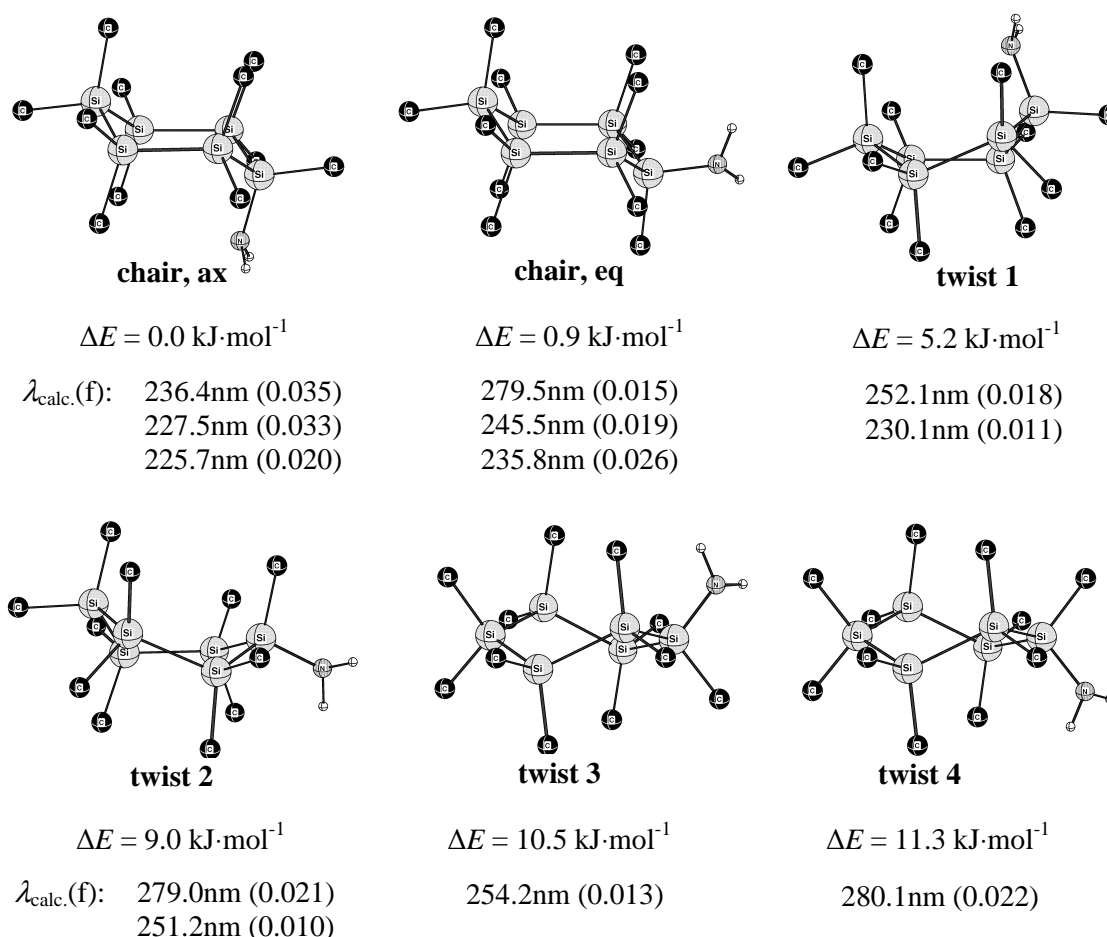


Fig. 6. DFT (B3LYP/6-31+G*)-optimized geometries, relative energies and time-dependent DFT B3LYP/TZVP UV long-wavelength absorption bands for **3** (oscillator strengths in parentheses).

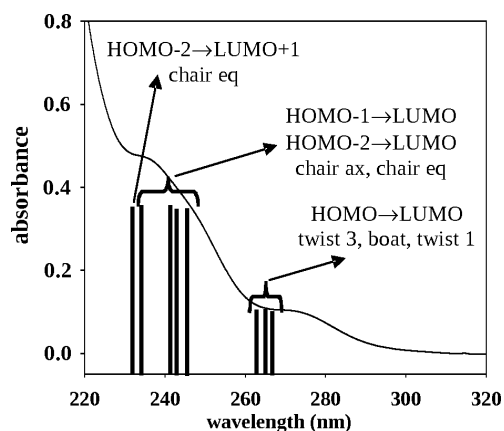


Fig. 7. Assignment of the experimental UV absorption spectrum by time-dependent DFT B3LYP/TZVP electron transitions for **2**, assuming contributions of different conformers.

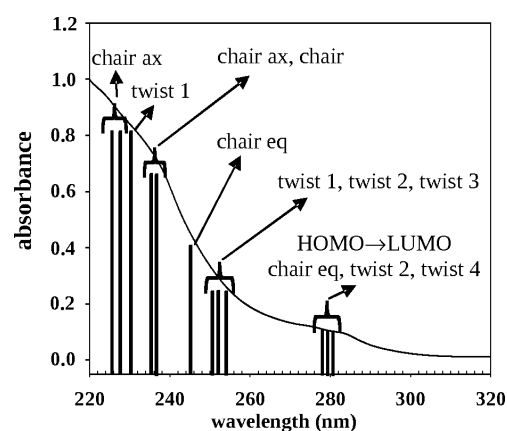


Fig. 8. Assignment of the experimental UV absorption spectrum by time-dependent DFT B3LYP/TZVP electron transitions for **3**, assuming contributions of different conformers.

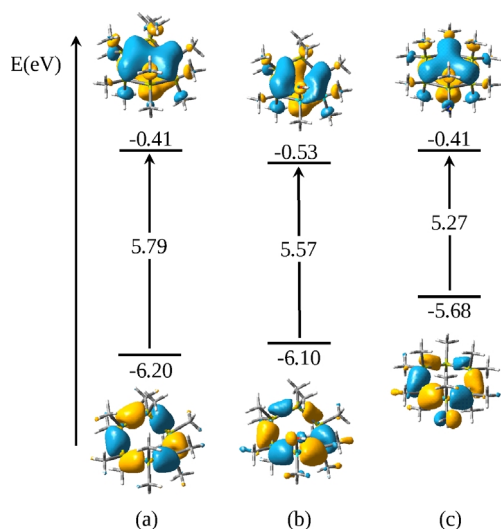


Fig. 9. Frontier orbital diagrams and calculated HOMO-LUMO gaps (GAUSSIAN 03; B3LYP/6-31+G*) for (a) *twist-1*, (b) *twist1-2* and (c) *chair,eq-3*.

26 nm red shift of the longest-wavelength UV absorption.

Conclusion

In summary, we have experimentally and theoretically investigated the structural and UV absorption characteristics of OH- and NH₂-substituted permethylcyclohexasilanes. At first it has been found that hydrogen bonding *via* the O-H groups can link the molecules into a cyclic trimer and thus to a considerable extent can influence the solid-state structure of otherwise unipolar molecules like cyclohexasilanol **2**. Furthermore, our results offer computational evidence that the experimental UV absorption spectra of cyclic oligosilanes also exhibit contributions of several conformers with very similar energies just as found earlier for their open-chained counterparts. Finally it has been shown that effective mixing of $\sigma(\text{Si-Si})$ and substituent lone pair orbitals are responsible for the substituent effects apparent in the UV absorption spectra of permethylcyclohexasilane derivatives.

Experimental Section

All experiments were performed under a nitrogen atmosphere using standard Schlenk techniques. Solvents were dried using a column solvent purification system [23]. NH₃ was dried by passing it through KOH and subsequent condensation onto Na. The cyclohexasilane derivatives Si₆Me₁₂ [24], and ClSi₆Me₁₁ [5f] were synthesized as previously

Table 2. Crystallographic data and structure refinement details for **2**.

Empirical Formula	C ₃₃ H ₁₀₂ Si ₁₈ O ₃
Formula weight	1052.77
Cryst. size, mm ³	0.36 × 0.28 × 0.20
Temperature, K	100(2)
Crystal system, space group	monoclinic, <i>P2₁/c</i>
<i>a</i> , Å	26.817(5)
<i>b</i> , Å	12.991(3)
<i>c</i> , Å	19.792(4)
β , deg	91.17(3)
<i>V</i> , Å ³	6894(2)
<i>Z</i>	4
<i>D</i> _{calcd} , g cm ⁻³	1.01
$\mu(\text{MoK}\alpha)$, mm ⁻¹	0.4
<i>F</i> (000), e	2304
Wavelength; λ , Å	MoK α ; 0.71073
θ range for data collection, deg	1.52–26.44
Limiting indices	–33 ≤ <i>h</i> ≤ 33, –16 ≤ <i>k</i> ≤ 15, –24 ≤ <i>l</i> ≤ 24
Reflections collected / unique / <i>R</i> _{int}	54310 / 14108 / 0.030
Completeness of θ , %	99.2
Max. / min. transmission	0.932 / 0.883
Data / restraints / parameters	14108 / 3 / 542
Final <i>R</i> 1/ <i>wR</i> 2 [<i>I</i> ≥ 2 σ (<i>I</i>)]	0.0332 / 0.0811
Final <i>R</i> 1/ <i>wR</i> 2 (all data)	0.0406 / 0.0846
GoF (<i>F</i> ²)	1.023
$\Delta\rho_{\text{fin}}$ (max / min), e Å ⁻³	0.51 / –0.18

reported. ¹H (300.13 MHz), ²⁹Si (59.62 MHz), and ¹³C (75.4 MHz) NMR spectra were recorded on a Bruker 300-MSL spectrometer in C₆D₆ solution *versus* external TMS. Mass spectra were run either on an HP 5971A/5890-II GC/MS coupling [HP 1 capillary column, length 25 m, diameter 0.2 mm, 0.33 μm poly(dimethylsiloxane)] or on a Kratos Profile mass spectrometer equipped with a solid probe inlet. Infrared spectra were obtained in Nujol mull on a Perkin-Elmer 883 spectrometer. UV/Vis spectra were recorded on a Perkin-Elmer Lambda 35 spectrometer. Melting points were determined using a Buechi apparatus according to Dr. Tottoli and are uncorrected. Elemental analyses were carried out on a Hanau Vario Elementar EL apparatus.

Hydroxyundecamethylcyclohexasilane (**2**)

A mixture of 8.24 g of Et₃N (81.5 mmol, 1.5 eq.), 50 mL of THF and 40 mL of H₂O was added to a solution of 20.06 g of ClSi₆Me₁₁ (54.31 mmol) in 100 mL of THF at 0 °C over a period of 1 h. The resulting mixture was allowed to warm to room temperature and stirred for another 3 h. After separation of the phases and extraction of the aqueous layer with three 30 mL portions of petroleum ether, the combined organic phases were dried over Na₂SO₄. Subsequent removal of the solvents and excess Et₃N *in vacuo* afforded 18.2 g of a crude product, which was purified by sublimation at 120 °C (0.02 mbar) to give 12.7 g (67 %) of **2** as a colorless, waxy solid. –²⁹Si NMR (C₆D₆, ext. TMS): δ = 13.63, –42.34, –42.74, –44.00 consistent with literature [9].

Aminoundecamethylcyclohexasilane (**3**)

Thoroughly dried NH₃ gas was slowly passed through a solution of 4.0 g (10.8 mmol) of ClSi₆Me₁₁ in 150 mL of pentane at r.t. for approximately 1 h, and subsequently stirred for an additional hour until complete conversion was achieved (reaction monitored by GC/MS). Filtration and removal of the solvent *in vacuo* gave 3.8 g of colorless crystals, from which 3.5 g (92%) of pure **3** could be obtained by recrystallization from pentane at -70 °C. M.p. 150 °C (dec.). – IR (Nujol mull): $\nu(\text{N-H}) = 3453$ (w), 3376 cm^{-1} (m). – ¹H NMR (C₆D₆, ext. TMS): $\delta = 0.361$ (s, 3H), 0.248 (s, 6H), 0.245 (s, 3H), 0.241 (s, 6H), 0.221 (s, 3H), 0.217 (s, 6H), 0.210 (s, 6H) (Si_{Ring}CH₃); -0.13 (b, 2H) (NH₂). – ¹³C NMR (C₆D₆, ext. TMS): $\delta = -0.49$ (H₂NSi_{Ring}CH₃), -5.88, -5.92, -5.94, -6.02, -6.18, -6.40 (Si_{Ring}(CH₃)₂). – ²⁹Si{¹H} NMR (C₆D₆, ext. TMS): $\delta = -15.26$ (Si_{Ring}MeNH₂), -42.27, -42.57, -44.11 (Si_{Ring}Me₂). – HRMS ((+)-ESI): $m/z = 348.13070$ (calcd. 348.12997 for C₁₁H₃₄NSi₆, [M+H]⁺).

Computational Methods

Structures were optimized at B3LYP/6-31+G* level using the GAUSSIAN 03 program package [25]. Analytical frequency calculations ensured the nature of the stationary points. The minima have only real frequencies while transition structures have exactly one imaginary frequency. For the electronic absorption spectra time-dependent B3LYP/TZVP calculations were performed with the program TURBOMOLE 5.7.1 [26]. Relative energies given include zero point vibrational energy (ZPVE) corrections.

X-Ray structure determination

Crystals of **2** were grown by cooling a pentane solution slowly to -30 °C. A suitable single crystal was mounted onto the tip of a glass fiber at -50 °C, and data collection was performed with a Bruker AXS Smart Apex CCD diffractometer using graphite-monochromatized MoK α radiation ($\lambda = 0.71073\text{ \AA}$). Crystal data and details of the data collection and structure refinement are summarized in Table 2. The data were reduced to F^2_o and corrected for absorption effects with the programs SAINT and SADABS [27]. The structure was solved by Direct Methods and refined by full-matrix least-squares (SHELXL-97 [28]). All non-hydrogen atoms were refined with anisotropic displacement parameters. The hydrogen atoms H(1), H(2) and H(3) belonging to the hydroxyl groups could be located in a difference Fourier map and were subsequently refined with a restrained O–H distance of 0.84 Å (SHELXL-97). All other hydrogen atoms were calculated to correspond to standard bond lengths and angles.

CCDC 734163 contains the supplementary crystallographic data for this paper. These data can be obtained free of charge from The Cambridge Crystallographic Data Centre via www.ccdc.cam.ac.uk/data_request/cif.

Acknowledgements

We thank the FWF (Wien, Austria) for financial support (project number P 17654-N19) and the Wacker Chemie GmbH (Burghausen, Germany) for the donation of silane precursors. Valuable support given by Dr. Roland Fischer is gratefully acknowledged.

- [1] For some reviews concerning the electronic properties of polysilanes, consult: a) C. G. Pitt in *Homoatomic Rings, Chains and Macromolecules of Main Group Elements*, (Ed.: A. L. Rheingold), Elsevier, New York, **1977**, p. 203; b) H. Sakurai, *J. Organomet. Chem.* **1980**, *200*, 261; c) H. Sakurai, *Pure Appl. Chem.* **1987**, *59*, 1637; d) R. D. Miller, J. Michl, *Chem. Rev.* **1989**, *89*, 1359; e) R. West in *Comprehensive Organometallic Chemistry II*, Vol. 2 (Eds.: G. Wilkinson, F. G. A. Stone, E. W. Abel), Pergamon Press, Oxford **1995**, p. 77; f) E. Hengge, H. Stueger in *The Chemistry of Organic Silicon Compounds*, Vol. 2 (Eds.: S. Patai, Z. Rappoport, Y. Apeloig), Wiley, Chichester, **1998**, p. 2177.
- [2] a) G. Mignani, M. Barzoukas, J. Zyss, G. Soula, F. Balegroune, D. Grandjean, D. Josse, *Organometallics* **1991**, *10*, 3660; b) D. Hissink, P. F. van Hutten, G. Hadziioannou, *J. Organomet. Chem.* **1993**, *454*, 25; c) H. K. Sharma, K. H. Pannell, I. Ledoux, J. Zyss, A. Ceccanti, P. Zanello, *Organometallics* **2000**, *19*, 770; d) C. Grogger, H. Rautz, H. Stueger, *Monatsh. Chem.* **2001**, *132*, 453.
- [3] a) H. Sakurai, H. Sugiyama, M. Kira, *J. Phys. Chem.* **1990**, *94*, 1837; b) M. Kira, T. Miyazawa, H. Sugiyama, M. Yamaguchi, H. Sakurai, *J. Am. Chem. Soc.* **1993**, *115*, 3116; c) M. Yamamoto, T. Kudo, M. Ishikawa, S. Tobita, H. Shizuka, *J. Phys. Chem. A* **1999**, *103*, 3144.
- [4] For reviews consult ref. [1a, d] and: H. A. Fogarty, D. L. Casher, R. Imhof, T. Schepers, D. W. Rooklin, J. Michl, *Pure Appl. Chem.* **2003**, *75*, 999.
- [5] a) D. N. Hague, R. H. Prince, *J. Chem. Soc.* **1965**, 4690; b) H. Gilman, W. H. Atwell, G. L. Schwabke, *J. Organomet. Chem.* **1964**, *2*, 369; c) H. Sakurai, S. Tasaka, M. Kira, *J. Am. Chem. Soc.* **1972**, *94*, 9285; d) C. G. Pitt, *J. Am. Chem. Soc.* **1969**, *91*, 6613; e) H. Stueger, E. Hengge, *Monatsh. Chem.* **1988**, *119*, 873; f) H. Stueger, G. Fuerpass, K. Renger, *Organometallics* **2005**, *24*, 6374.

- [6] a) R. West in *The Chemistry of Organic Silicon Compounds*, Vol. 3 (Eds.: Z. Rappoport, Y. Apeloig), Wiley, Chichester, **2001**, p. 541; b) H. Tsuji, J. Michl, K. Tamao, *J. Organomet. Chem.* **2003**, *685*, 9.
- [7] a) D. W. Rooklin, T. Schepers, M. K. Raymond-Johansson, J. Michl, *Photochem. Photobiol. Sci.* **2003**, *2*, 511; b) B. Albinsson, H. Teramae, J. W. Downing, J. Michl, *Chem. Eur. J.* **1996**, *2*, 529.
- [8] G. Tekautz, A. Binter, K. Hassler, M. Flock, *Chem. Phys. Chem.* **2006**, *7*, 421.
- [9] E. Hengge, M. Eibl, *J. Organomet. Chem.* **1989**, *371*, 137.
- [10] D. Kovar, K. Utvary, E. Hengge, *Monatsh. Chem.* **1979**, *110*, 1295.
- [11] H. L. Carrell, J. Donohue, *Acta Crystallogr.* **1972**, *28B*, 1566.
- [12] a) M. E. Straumanis, E. Z. Aka, *J. Appl. Phys.* **1952**, *23*, 330; b) A. Spielberger, P. Gspaltl, H. Siegl, E. Hengge, *J. Organomet. Chem.* **1995**, *499*, 241; c) A. A. Korlyukov, D. Y. Larkin, N. A. Chernyavskaya, M. Y. Antipin, A. I. Chernyavskii, *Mendeleev Comm.* **2001**, 195; d) D. Y. Larkin, A. A. Korlyukov, E. V. Matukhina, M. I. Buzin, N. A. Chernyavskaya, M. Y. Antipin, A. I. Chernyavskii, *Russ. Chem. Bull. Int. Ed.* **2005**, *54*, 1612.
- [13] P. D. Lickiss, *Adv. Inorg. Chem.* **1995**, *42*, 147.
- [14] V. Chandrasekhar, R. Boomishankar, S. Nagendran, *Chem. Rev.* **2004**, *104*, 5847.
- [15] a) M. Dräger, K. G. Walter, *Z. Anorg. Allg. Chem.* **1981**, *479*, 65; b) K. Kumar, M. H. Litt, R. K. Chada, J. E. Drake, *Can. J. Chem.* **1987**, *65*, 437; c) H. Rautz, H. Stueger, G. Kickelbick, C. Pietzsch, *J. Organomet. Chem.* **2001**, *627*, 167.
- [16] V. Chandrasekhar, S. Nagendran, R. J. Butcher, *Organometallics* **1999**, *18*, 4488.
- [17] L. F. Brough, R. West, *J. Am. Chem. Soc.* **1972**, *94*, 9285.
- [18] H. Stueger, E. Hengge, *Monatsh. Chem.* **1988**, *119*, 873.
- [19] C. G. Pitt, *J. Am. Chem. Soc.* **1969**, *91*, 6613.
- [20] J. R. Koe, M. Motonaga, M. Fujiki, R. West, *Macromolecules* **2001**, *34*, 706.
- [21] See ref. [1e], and refs. cited therein.
- [22] a) K. Takeda, K. Shiraishi, *Solid State Commun.* **1993**, *85*, 301; b) Y. L. Hsiao, R. M. Waymouth, *J. Am. Chem. Soc.* **1994**, *116*, 9779.
- [23] A. B. Pangborn, M. A. Giardello, R. H. Grubbs, R. K. Rosen, F. J. Timmers, *Organometallics* **1996**, *15*, 1518.
- [24] E. Carberry, R. West, *J. Am. Chem. Soc.* **1969**, *91*, 5440.
- [25] M. J. Frisch, G. W. Trucks, H. B. Schlegel, G. E. Scuseria, M. A. Robb, J. R. Cheeseman, J. A. Montgomery, Jr., T. Vreven, K. N. Kudin, J. C. Burant, J. M. Millam, S. S. Iyengar, J. Tomasi, V. Barone, B. Menonucci, M. Cossi, G. Scalmani, N. Rega, G. A. Petersson, H. Nakatsuji, M. Hada, M. Ehara, K. Toyota, R. Fukuda, J. Hasegawa, M. Ishida, T. Nakajima, Y. Honda, O. Kitao, H. Nakai, M. Klene, X. Li, J. E. Knox, H. P. Hratchian, J. B. Cross, C. Adamo, J. Jaramillo, R. Gomperts, R. E. Stratmann, O. Yazyev, A. J. Austin, R. Cammi, C. Pomelli, J. W. Ochterski, P. Y. Ayala, K. Morokuma, G. A. Voth, P. Salvador, J. J. Dannenberg, V. G. Zakrzewski, S. Dapprich, A. D. Daniels, M. C. Strain, O. Farkas, D. K. Malick, A. D. Rabuck, K. Raghavachari, J. B. Foresman, J. V. Ortiz, Q. Cui, A. G. Baboul, S. Clifford, J. Cioslowski, B. B. Stefanov, G. Liu, A. Liashenko, P. Piskorz, I. Komaromi, R. L. Martin, D. J. Fox, T. Keith, M. A. Al-Laham, C. Y. Peng, A. Nanayakkara, M. Challacombe, P. M. W. Gill, B. Johnson, W. Chen, M. W. Wong, C. Gonzalez, J. A. Pople, GAUSSIAN 03 (Rev. C.02), Gaussian, Inc., Wallingford CT (USA) **2004**.
- [26] a) R. Ahlrichs, M. Bär, M. Häser, H. Horn, C. Kölmel, *Chem. Phys. Lett.* **1989**, *162*, 165; b) A. Schäfer, C. Huber, R. Ahlrichs, *J. Chem. Phys.* **1994**, *100*, 5829; c) R. Bauernschmitt, R. Ahlrichs, *Chem. Phys. Lett.* **1996**, *256*, 454; d) R. Bauernschmitt, M. Häser, O. Treutler, R. Ahlrichs, *Chem. Phys. Lett.* **1997**, *264*, 573.
- [27] a) SAINT+ (version 6.45), Software Reference Manual, Bruker Analytical X-ray Instruments Inc., Madison, WI (USA) **1997–2003**; b) SADABS, Program for Empirical Absorption Correction of Area Detector Data, Bruker Analytical X-ray Instruments Inc., Madison, WI (USA) **1998**.
- [28] G. M. Sheldrick, SHELXL-97, Program for the Refinement of Crystal Structures, University of Göttingen, Göttingen (Germany) **1997**. See also: G. M. Sheldrick, *Acta Crystallogr.* **2008**, *A64*, 112.